Environmental Science & Technology

pubs.acs.org/est

Article

Deep-Learning-Based Automated Tracking and Counting of Living Plankton in Natural Aquatic Environments

Zhuo Chen, Meng Du, Xu-Dan Yang, Wei Chen, Yu-Sheng Li, Chen Qian,* and Han-Qing Yu*

Cite This: https://doi.org/10.1021/acs.est.3c00253

Read Online

ACCESS | Metrics & More | Article Recommendations | Supporting Information

ABSTRACT: Plankton are widely distributed in the aquatic environment and serve as an indicator of water quality. Monitoring the spatiotemporal variation in plankton is an efficient approach to forewarning environmental risks. However, conventional microscopy counting is time-consuming and laborious, hindering the application of plankton statistics for environmental monitoring. In this work, an automated video-oriented plankton tracking workflow (AVPTW) based on deep learning is proposed for continuous monitoring of living plankton abundance in aquatic environments. With automatic video acquisition, background calibration, detection, tracking, correction, and statistics, various types of moving zooplankton and phytoplankton were counted at a time scale. The accuracy of AVPTW was validated with conventional counting via microscopy. Since AVPTW is only sensitive to mobile plankton, the temperature- and wastewater-discharge-induced plankton population variations were monitored online, demonstrating the sensitivity of AVPTW to environmental changes. The robustness of AVPTW was also confirmed with natural water samples from a contaminated river and an uncontaminated lake. Notably, automated workflows are essential for generating large amounts of data, which are a prerequisite for available data set construction and subsequent data mining. Furthermore, data-driven approaches based on deep learning pave a novel way for long-term online environmental monitoring and elucidating the correlation underlying environmental indicators. This work provides a replicable paradigm to combine imaging devices with deep-learning algorithms for environmental monitoring.

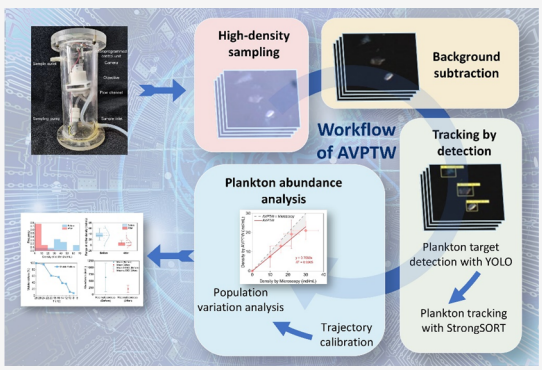

KEYWORDS: *environmental monitoring, plankton abundance, deep learning, tracking, detection, aquatic environment*

INTRODUCTION

As a vital component in the aquatic environment, plankton play a pivotal role in the flow of energy through ecosystem nutrients and carbon cycling[1−3] and provide early warning signs of risky environmental changes.[4] Previous studies have revealed the correlations between water quality and plankton, including zooplankton and phytoplankton. Zooplankton respond to changes in the aquatic environment quickly and sensitively,[5−7] and phytoplankton (including eukaryotic algae and cyanobacteria) are largely associated with eutrophication and harmful algal blooms.[8,9] Therefore, monitoring the spatiotemporal variation in plankton abundance is an efficient way to capture changes in water quality.[10−12] The strategies for phytoplankton counting had been developed by 1989,[13] but the conventional microscopy counting is time-consuming and requires specialized experts and subjectivity of classification.[14] Therefore, massive statistical information acquisition and long-term monitoring of ecological conditions via tracking and counting living plankton in aquatic environments remain a great challenge.

Recently, success in object detection based on deep learning makes rapid, real-time, cost-effective, and labor-free tools a reality. Deep-learning-based image recognition techniques have been applied in environmental monitoring and management, such as scattered garbage regions,[15] fish biodiversity monitoring,[16] and plankton identification.[17−19] Several devices, including Dual Scripps Plankton Camera (DSPC),[14,20] FlowCam,[21] ZooScan,[22] and FlowCytobot,[23] were developed to monitor planktonic organisms and help to image and identify plankton. Although in these studies deep learning was introduced into plankton observation, these image-based monitoring methods have several weaknesses in applications. First, different living plankton look similar. As a result, misclassification might occur with a single image. Second, if the morphology of plankton remains unchanged due to acute toxicity or death, the impact of acute environmental change or pollution cannot be detected. Hence, a gap between plankton detection and using plankton as indicators in aquatic environments remains. Characteristics of plankton and

Special Issue: Data Science for Advancing Environmental Science, Engineering, and Technology

Received: January 10, 2023
Revised: April 13, 2023
Accepted: May 5, 2023

requirements of deep learning increase the difficulty in plankton tracking and counting: e.g., difficulty in mobile zooplankton counting. Previous studies focused on plankton recognition and detection under discontinuous frames, ignoring the motion information underlying continuous frames.

In this work, we propose a new approach with a focus on the association of targets between continuous frames and achieve the quantification of multiclass swimming plankton. Introducing plankton motion as a new dimension, an automated video-oriented plankton tracking workflow (AVPTW) for plankton flowing sampling and statistical analysis was developed. With a continuous sampling device and tracking-by-detection method, long-term continuous automated plankton statistics were achieved. Then, AVPTW was compared with the conventional microscopic counting results to verify the reliability of AVPTW and evaluate the performance of our data analysis framework. Subsequently, the sensitivity of AVPTW was examined with temperature-induced rotifer population variation. Finally, plankton in a contaminated river and an uncontaminated lake were monitored, and the effects of industrial wastewater discharge on zooplankton were simulated. In addition, efforts were made to improve the identification of small plankton, including tracking-by-detection, data augmentation, and input image size, thus providing an example for the joint use of machine-learning and deep-learning algorithms.

MATERIALS AND METHODS

Workflow of AVPTW. The workflow includes the following four steps: first, massive continuous videos were collected with a homemade continuous injection device, followed by background calibration; second, plankton were detected with the YOLO (You Only Look Once)[24,25] model; next, multiple plankton were tracked using StrongSORT;[26] finally, trajectories were calibrated and statistically analyzed for plankton population variation identification. The specific steps of the workflow are illustrated in Figure 1.

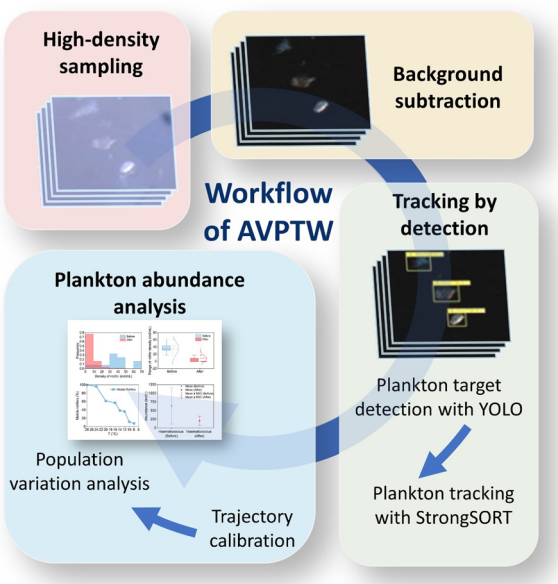

Figure 1. Workflow of AVPTW.

Data Collection with Continuous Injection Device. A homemade continuous injection device, consisting of a microprogrammed control unit, camera, objective, autosampling pump, and flow channel, was fabricated (Figure S1). Water samples flowed into the flow channel driven by the pump. While keeping the same appearance and motility as usual under natural conditions, zooplankton and phytoplankton were confined into the observation area for continuous data acquisition. After acquisition, the aquatic sample was automatically replaced by the next batch of aquatic samples in the continuous injection device. The specific parameters of the sampling process are given below. The sampling duration for each sample was 3 s, and detection duration was 10 s, 20 or 30 s. The automatic sampling frequency of this device could be adjusted on demand: 5 min per sampling for long-term monitoring frequency and 2 min per sampling for short-term monitoring frequency.

Data Preprocessing. Impurities such as particulate matter and microplastics are widespread in aquatic environments with sizes comparable to those of zooplankton. Their existence possibly leads to unfavorable observation conditions, such as occlusion, background clutter, and shading.[27] To avoid the impact of these materials on detection accuracy, the collected videos were subtracted from the median background. The process of background subtraction was composed of several detailed steps. First, the median values of the red (R), green (G) and blue (B) channels of all pixels for the entire frames of a video were computed, and the median was considered as the median background. Second, each frame subtracted the median background, and any resulting negative values were clipped to zero. Third, the obtained values were rescaled to the interval of (0, 255), and the processed frames were overwritten to the video. Zooplankton and phytoplankton in videos could be observed more clearly after background calibration.

Data Set Preparation Combined Data Augmentation. A total of 3307 images containing zooplankton and phytoplankton were manually marked with bounding boxes and classes. To focus on zooplankton and phytoplankton related to the environment, the choice of the classes depended on their relevance to water quality and principles of taxonomy. Based on the investigation into the local environmental water samples, Parameciidae, Euglenidae, Trachelophyllidae, Litonotidae, Rotifer, and Haematococcus were selected.

Prior to data augmentation, the data set (3307 images) was divided into a training set (2977 images) and a test set (330 images). Here, the size of the training set increased 10-fold from 2707 to 27070 by an off-the-shelf tool (https://github.com/cuitno1/Data-enhancement and https://github.com/maozezhong/CV_ToolBox/tree/master/DataAugForObjectDetection). The tool provided small data sets with support for data augmentation, implemented by random multiple variations in existing images and labels. The approaches used in this tool consisted of crop, shift, flip, noise addition, light change, and cutout. In particular, cutout efficiently increased the generalization capability of the model by simulating occluded instances.[28]

Likewise, the rational composition of the data set needed to be taken into account. A total of 270 unlabeled background images were then added into the data set, improving the model by reducing the false positives (FP). Background images offered instances of impurities that could cause confusion with the targeted object.

https://doi.org/10.1021/acs.est.3c00253
Environ. Sci. Technol. XXXX, XXX, XXX−XXX

Evaluation of Training Methods. In data set preparation and training, three approaches were compared to seek better training methods: (i) with and without data augmentation, (ii) number of parameters for pretrained models, and (iii) image sizes set at 1280 pixels and 640 pixels. Herein, image size represented image resolution, which indicates the size of images input to the network. YOLOv5s, YOLOv5m, YOLOv5s6, and YOLOv5m6 were all pretrained models of YOLOv5 for mobile deployments. The image size was set at 640 pixels for YOLOv5s and YOLOv5m, while it was set at 1280 pixels for YOLOv5s6 and YOLOv5m6. YOLOv5m has more parameters and higher accuracy but lower speed than those of YOLOv5s, and the relationship is the same as that between YOLOv5m6 and YOLOv5s6. Six types of methods were obtained, including YOLOv5m6 + data augmentation (YOLOv5m6 + DA), YOLOv5s6 + data augmentation (YOLOv5s6 + DA), YOLOv5m6, YOLOv5s6, YOLOv5m and YOLOv5s. Among these, only YOLOv5m6 +DA and YOLOv5s6 + DA expanded the data set by means of the data augmentation previously mentioned.

Multiple Object Tracking Based on StrongSORT. Since motion and appearance variations of mobile zooplankton might cause loss of frames in detection and inaccuracy of the quantity count, StrongSORT combined with YOLO was used for multiple classes tracking-by-detection.[29] In contrast to the region-based detectors such as Fast R-CNN,[30] YOLO's one-stage detector enables real-time inference, thereby enhancing the efficiency of detecting plankton. Furthermore, YOLO is a widely used mainstream detection algorithm that require less computing power and storage space than region-based detectors like Fast R-CNN. YOLO's lightweight nature also facilitates deployments on edge devices. Unlike the pedestrian and car trajectories for which StrongSORT was successfully used, the tracks of zooplankton and phytoplankton were possibly diverse and nonlinear. In some cases, the identity (ID) of some targets even changed due to the miscalculation of the tracking algorithm, leading to inaccuracy of zooplankton and phytoplankton counting. Therefore, in addition to using an off-the-shelf ImageNet pretrained model for our categories, an ID rearrangement strategy was also used. First, each existing ID was recorded in the ID sequence after tracking. Next, it was determined whether the target ID had appeared in the existing ID sequence. Finally, according to the result, a new ID for the target was assigned. Image processing and tracking were carried out on a server with an NVIDIA GeForce GTX 3090 GPU and a 3.50 GHz Intel Core i9-10920X CPU. All codes were compiled in MATLAB R2021a and Python 3.8.13.

Evaluation Criteria. Commonly used criteria for object detection include precision (p), recall (r), AP50, mAP, and F1-score. These criteria can be defined as follows:

$$\text{precision} = \frac{\text{TP}}{\text{TP} + \text{FP}} \tag{1}$$

$$\text{recall} = \frac{\text{TP}}{\text{TP} + \text{FN}} \tag{2}$$

$$\text{average precision (AP)} = \int_0^1 p(r)\,\mathrm{d}r$$

$$\text{AP50 is AP at IoU} = 0.50 \tag{3}$$

$$\text{mAP} = \frac{1}{\text{classes number}} \sum_{\text{i}}^{\text{classes number}} \text{average precision} \tag{4}$$

$$\text{F1} = 2 \times \frac{\text{precision} \times \text{recall}}{\text{precision} + \text{recall}} \tag{5}$$

True positives (TP) in the formula refer to the number of targets correctly detected as positive. FP means the number of misclassified positive targets. False negative (FN) is the number of misclassified negative targets. Intersection over Union (IoU) represents the overlap level of the ground truth and bounding box. Since precision and recall are usually inversely proportional, another metric is needed for model evaluation. F1-score and mAP are principal evaluation indicators to measure the integrated performance of object identification. mAP@.5 and mAP@.5:.95 refer to mAP at IoU = 0.5 and IoU = 0.5, 0.55, 0.6, 0.65, 0.7, 0.75, 0.8, 0.85, 0.9, 0.95, respectively.

Quantitative Ability Verification Experiment. Paramecium was extracted from the lake. After one to 2 weeks of incubation, solutions containing paramecium were diluted to one-fourth, half, and three-fourths of the original solution. In these samples, the densities of the paramecium were calculated by manual microscopy counting and AVPTW.

Robustness of AVPTW for Natural Water Samples. Three meaningful sites of Nanfei River (Hefei City, China), a contaminated river, were investigated, including a site near the upstream wastewater outlet (site 1), 3 km downstream (site 2), and 7.6 km downstream (site 3). A 25# plankton net (pore size: 0.064 mm) was applied to concentrate zooplankton and phytoplankton in the samples. All samples were collected on the same day at a temperature of 20−23 °C. After collection, all samples were detected by an automatic detection work flow in 24 h.

To comprehensively characterize the samples, the water samples from different sites were also measured by a fluorescence excitation−emission matrix (EEM) with a fluorescence spectrophotometer (Aqualog, Horiba Co., Japan) and chemical oxygen demand (COD, fast digestion-spectrophotometric method).

Temperature-Induced Zooplankton Population Variation. Since rotifers are sensitive to temperature, they were selected as the experimental subject, and temperature was chosen as the regulated environmental condition. The freshwater rotifers used in this work contained normal species, such as *Brachionus calyciflorus*, *Rotifer vulgaris*, and *Lepadella patella*. Before the experiment, the rotifer solution was placed at 28 °C. When the water temperature gradually decreased from 28 to 8 °C in an ice bath, the rotifer population in the solution was counted with our automatic detection device. The entire process was completed in 80 min to avoid motility recovery for rotifers. In the cooling process, 36 videos (containing 10800 frames) were acquired. Mobile rotifers were used to evaluate the effect of temperature on rotifer motility, referring to the proportion of swimming rotifers in the total number of rotifers.

Simulation of Industrial Water Discharge. Concentrated samples (5-fold concentration) from the Nanfei River and original samples collected from Yanjing Lake at our campus were tested. The former denotes a single class with high abundance, and the latter denotes a multiclass with low abundance. After examining the original density of the unprocessed samples with AVPTW for 22−312 min, a volume of 0.25 mL of industrial wastewater from an industrial park in Shandong Province, China, with a COD of approximately 6500 mg/L was added to 50 mL samples at a concentration of 0.5%

https://doi.org/10.1021/acs.est.3c00253
Environ. Sci. Technol. XXXX, XXX, XXX−XXX

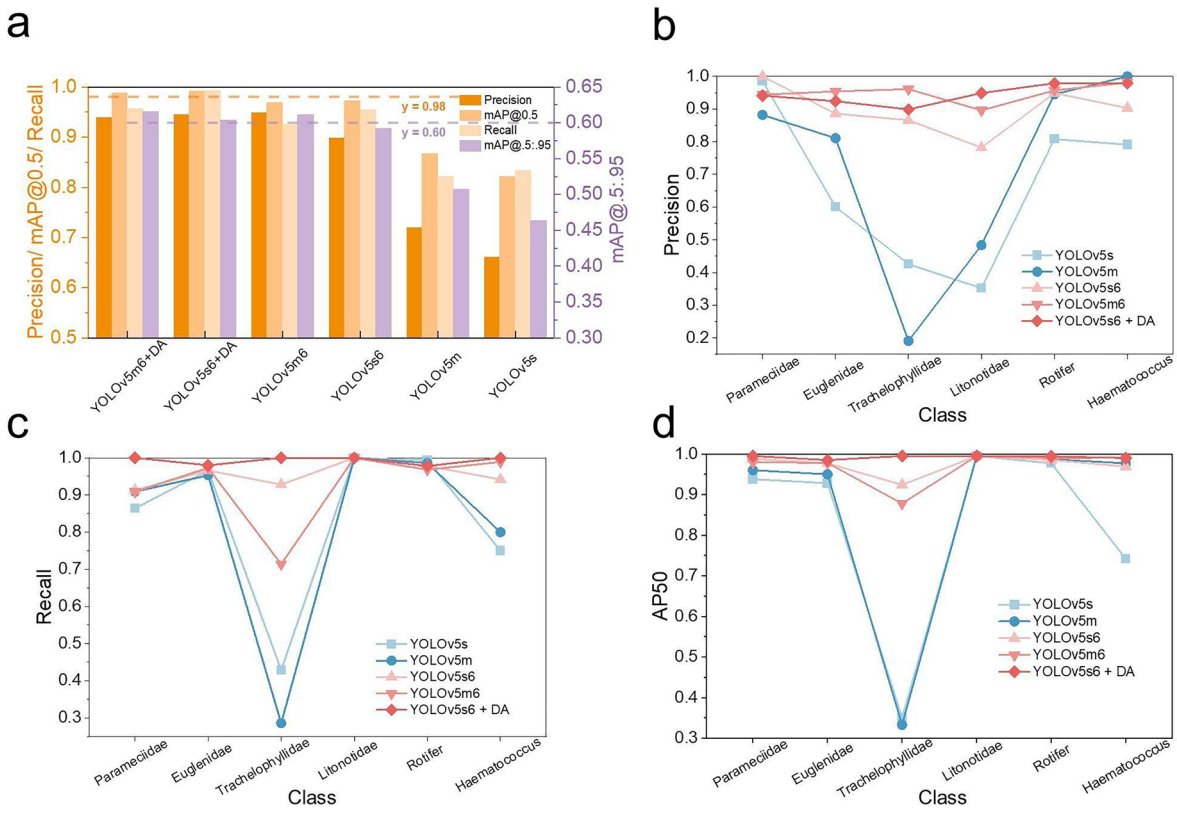

Figure 2. Evaluation criteria for the models trained by different methods: (a) precision, recall, mAP@0.5, and mAP@.5:.95 on average for all classes, (b) precision for each class, (c) recall for each class, and (d) AP50 for each class. The training methods include YOLOv5m6 + DA, YOLOv5s6 + DA, YOLOv5m6, YOLOv5s6, YOLOv5m, and YOLOv5s.

to simulate sudden contamination. After dosing industrial wastewater, the samples were continuously examined by AVPTW for 373 min to 24 h.

RESULTS AND DISCUSSION

Data Augmentation and Model Optimization. Precision, recall, mAP, and F1-score were used to evaluate the detection efficiency of models trained on different pretrained models and data sets (Figure 2). Figure 2a shows an overview of the performance of different methods. As expected, YOLOv5s6 + DA had the highest precision (0.945), recall (0.993), and mAP@0.5 (0.992). Although YOLOv5m6 and YOLOv5s6 also performed well, both of them had individual indicators slightly inferior to those of YOLOv5s6 + DA. The difference shows that data augmentation contributed to the overall metrics. Apparently, YOLOv5s6 + DA, YOLOv5m6, and YOLOv5s6 performed better than YOLOv5m and YOLOv5s. These results demonstrate that a larger image size led to a better performance on average for all classes. Nevertheless, no significant difference was found between YOLOv5m and YOLOv5s, revealing that improvement brought by pretrained models was smaller than was expected. Similar findings were concluded from the comparison of F1-score (Table 1).

Table 1. F1-Score of the Models Trained in the Different Methods for the Average of All Classes

method	F1-score (%)
YOLOv5s6 + DA	96.84
YOLOv5m6	93.74
YOLOv5s6	92.56
YOLOv5m	76.71
YOLOv5s	73.75

A further analysis of the evaluation indicators in each category was conducted. As expected, AP50 of YOLOv5s6 + DA for all classes was over 0.95, which achieved the best results among all methods (Figure 2d). Comparing the data of YOLOv5s6, data enhancement resulted in a significant increase in average precision. Apparently, YOLOv5s6 + DA, YOLOv5m6, and YOLOv5s6 performed better than YOLOv5m and YOLOv5s for most classes (Figure 2b–d). Trachelophyllidae and Litonotidae were regarded as rare classes because of the small sample size in the data set. What stands out in Figure 2 is the difference in performance between image size 1280 pixels and 640 pixels for rare classes. Furthermore, analysis of the consistency of prediction and labeling results for each class and for different methods can be seen in the confusion matrix (Figure S2) and batch of the validation set (val batch) comparison (Figures S3–S5). For small plankton detection, this discrepancy could be attributed to more efficient features learned in the network after larger-size images were fed into the network. Herein, data augmentation and an image size of 1280 pixels were considered as practical methods for improving performance. These approaches might also be effective for other tasks with small target detection, helping us to optimize the strategies for data training in time-consuming deep-learning tasks, especially the joint use of deep-learning algorithms involving complex parameters and frameworks. Owing to the larger number of model parameters in YOLOv5m6, the training and predicting time for YOLOv5m6

https://doi.org/10.1021/acs.est.3c00253
Environ. Sci. Technol. XXXX, XXX, XXX−XXX

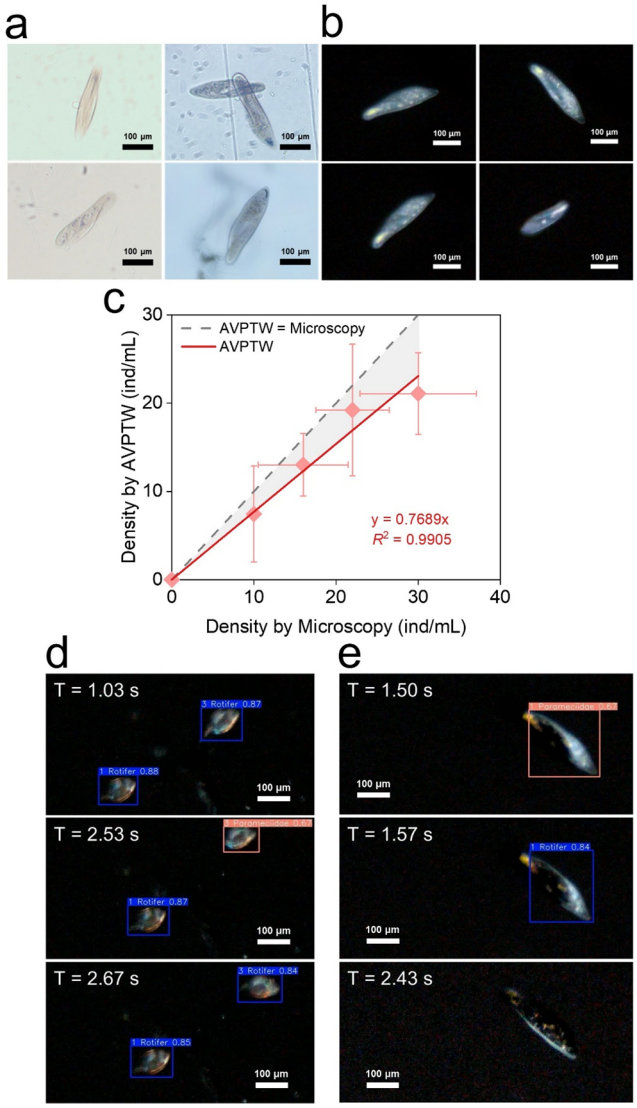

Figure 3. (a) Paramecium observed by microscopy. (b) Preprocessed images of paramecium captured by AVPTW. (c) Density counted by microscopy and AVPTW. (d) Misidentification of rotifer as paramecium. (e) Misidentification of paramecium as rotifer.

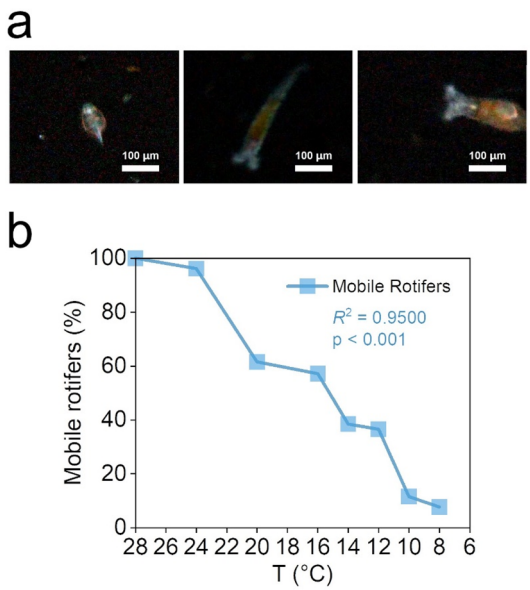

Figure 4. Rotifer appearance and temperature-induced rotifer counting variation with AVPTW: (a) preprocessed images of rotifers captured by AVPTW and (b) variation in mobile rotifers with temperature.

+ DA was longer compared to YOLOv5s6 + DA. However, since YOLOv5s6 + DA achieved satisfactory performance (Figure 2a), the use of a more time-consuming model is unnecessary. These results suggest that the performance of YOLOv5s6 with data augmentation is already sufficient for the purpose of plankton detection in this study; thus, YOLOv5s6 + DA was used for the subsequent experiment. For per image containing living plankton, the prediction part spent 10−21 ms with YOLO and the tracking part spent 22−33 ms with StrongSORT. The proximity to real-time identification indicates that sampling equipment and analytical models can be integrated and deployed to intelligent edge devices at extremely low hardware costs.

Visualization of target features extracted by the model contributes to understanding how artificial intelligence realizes a detection task and reveals the interaction of features.[31] As an example, a frame where an instance of Parameciidae was detected was presented (Figure S17). The features from different layers focus on different profiles or overall information. Interestingly, shallow features tended to be more complete than deep features, while deep features tended to be more detailed and smaller than shallow features. Different features were highly correlated with each other and together contributed to the overall plankton detection (Figure S17c−f).

Validation of the Quantitative Ability of AVPTW. The ability of our automated workflow to detect and count zooplankton accurately was further confirmed with manual counting via a microscope. In the videos collected by the automatic detection device, the appearances and colors of paramecium could be clearly distinguished from the background (Figure 3a,b). Thus, colorful and high-contrast images lessened the difficulty of labeling and detection.

An R^2 value of 0.9905 reveals the positive correlation between the counts obtained by the automated track workflow and the actual concentration (Figure 3c), indicating that the automated counting results were reliable. Notably, the counts of AVPTW were lower than those of microscopy, which might be explained by counting deviation due to the swimming of the paramecium in microscopic observation. However, the throughput of AVPTW was higher than that of counting via microscopy, making the deviation in the counts in a single injection negligible for the statistical analysis. The linear relationship between the counts of AVPTW and microscopy demonstrates the accuracy of counting results compared with the manual counting method, indicating that AVPTW has a great potential for the quantitative analysis of plankton in aquatic environments.

In addition to counting reliability, two significant advantages of the automated track workflow, convenience and stability, were also demonstrated. On the one hand, due to strong mobility, the distribution of paramecium was usually uneven in water, making microscopic counting time- and labor-consuming. By comparison, our imaging device collected 4200 frames automatically and conveniently. On the other hand, posture changes occurred in the motion of paramecium, causing misclassification in image-based analysis[32] and

https://doi.org/10.1021/acs.est.3c00253
Environ. Sci. Technol. XXXX, XXX, XXX−XXX

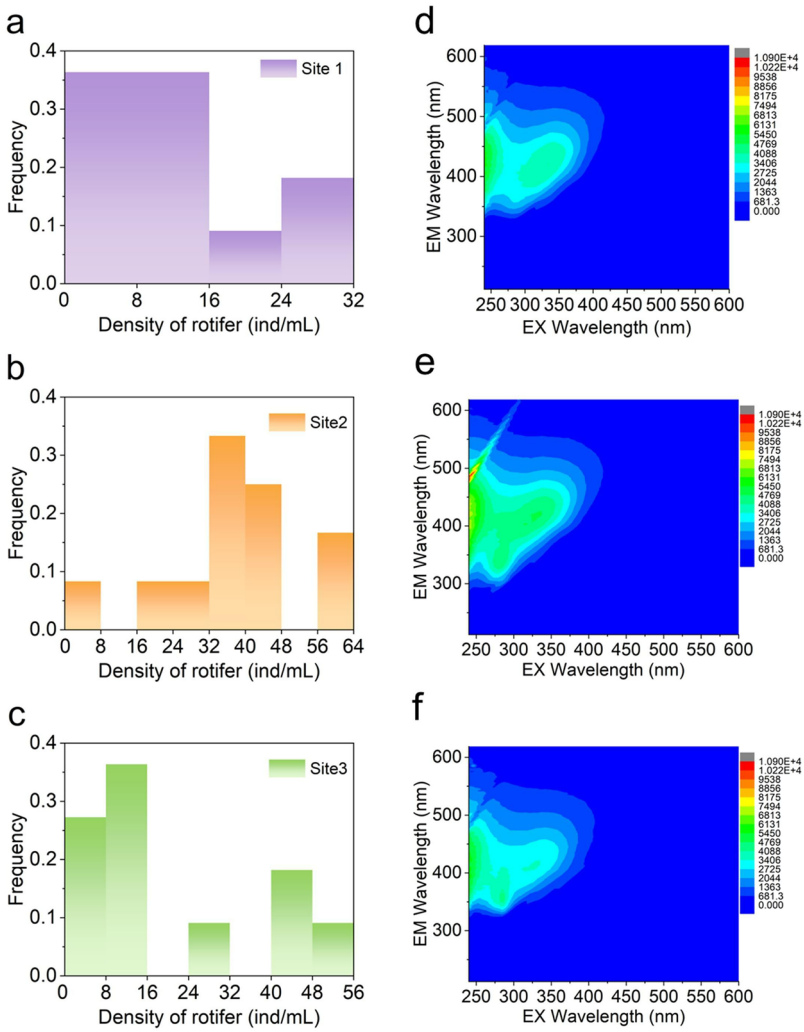

Figure 5. Characteristics of the water samples from Nanfei River. Rotifer density of (a) Site 1, (b) Site 2, and (c) Site 3. Fluorescence EEMs of (d) Site 1, (e) Site 2, and (f) Site 3.

inaccurate counting. For example, the rotifer might be misidentified as paramecium in some frames when using YOLO and StrongSORT only (Figure 3d,e, Supporting Movies 1 and 2). If only a single image was analyzed, misidentification might lead to the statistical result. However, since AVPTW was associating plankton across video frames using multiobject tracking and calibrating IDs to generate complete moving trajectories, the misidentification could be corrected.[33] Altogether, this result demonstrates that this automated track workflow could provide a stable and efficient approach for microbiology testing.

Continuous Monitoring of the Temperature-Induced Zooplankton Counting Variation. There is a pronounced connection between rotifer motility and shifts in temperature, and rotifers would become immobilized temporarily if the temperature dropped from 20 to 8 °C.[34] Therefore, the sensitivity of AVPTW to temperature should be validated for continuous monitoring. Freshwater rotifers consist of multiple species with different shapes, sizes and speeds, making it challenging to classify and track them as one class of "Rotifer". With our AVPTW, freshwater rotifers in multiple species, such as *Brachionus calyciflorus*, *Rotifer vulgaris* and *Lepadella patella*, could be identified successfully (Figure 4a), demonstrating that this automated track workflow could identify and track highly variable instances of the same class. Therefore, the adequate data sets and tracking framework provided an effective solution to the mentioned problem.

As the temperature declined from 28 to 24 °C, swimming rotifers were reduced by only 3.85% (Figure 4b). Interestingly, a drastic drop in 40.64% in mobile rotifers was observed after the temperature was reduced from 24 to 16 °C, indicating that such a reduction temporarily incapacitated a substantial portion of rotifers. When the temperature was further dropped to 8 °C, swimming rotifers continued to decrease. Notably, below 8 °C, there was a 92.31% reduction in mobile rotifers compared with that at 28 °C, suggesting that low temperature temporarily and severely disrupted rotifer locomotion. Consistent with previous reports,[34] these findings provide evidence for perturbations in temperature on rotifer motility. This consistency also served as compelling evidence for the precision and validity of statistical analysis, again confirming the ability of AVPTW to continuously monitor zooplankton counting variation. The applications of AVPTW could also be extended for monitoring the effects of other common natural environmental factors on plankton activity, such as pH, dissolved oxygen, and nutrients.

Robustness of AVPTW for Natural Samples. After the above results confirmed the effectiveness of AVPTW in

https://doi.org/10.1021/acs.est.3c00253
Environ. Sci. Technol. XXXX, XXX, XXX−XXX

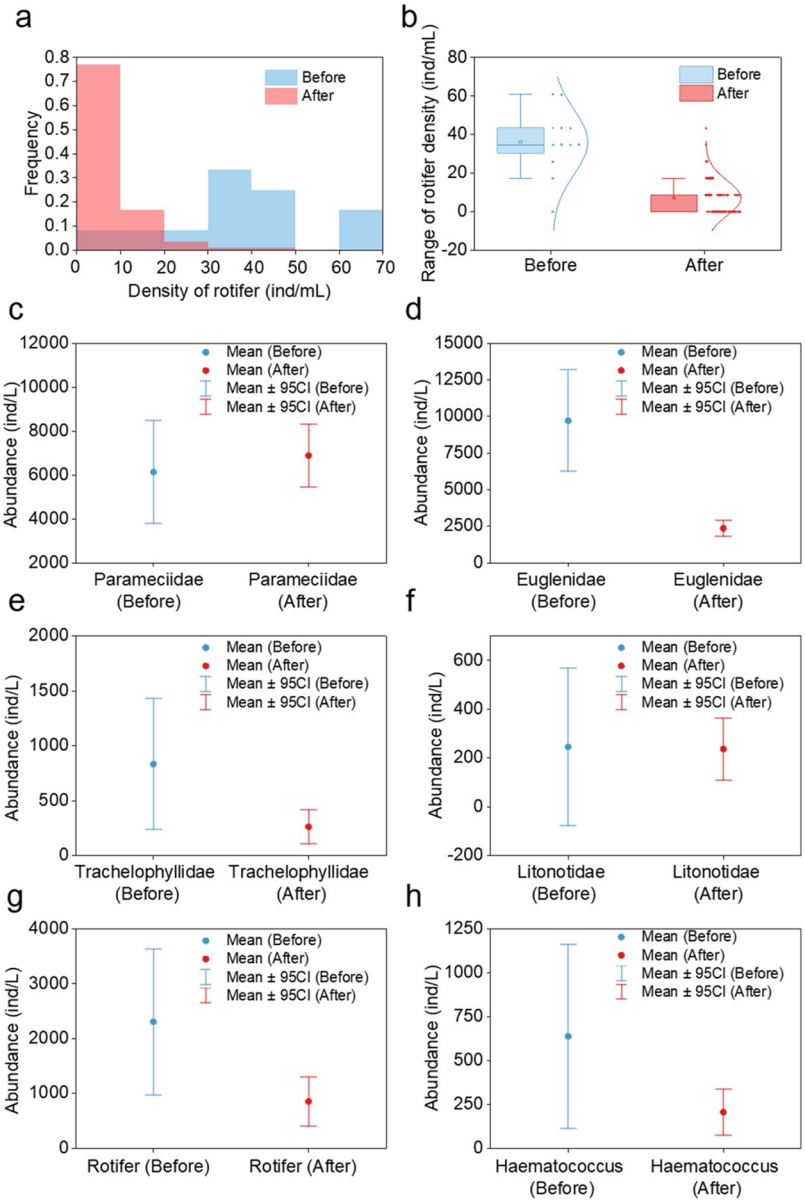

Figure 6. Plankton density of the water samples before and after dosing industrial wastewater: (a) rotifer density and frequency and (b) range of rotifer density in Nanfei River. (c) Parameciidae, (d) Euglenidae, (e) Trachelophyllidae, (f) Litonotidae, (g) Rotifer, and (h) Haematococcus in Yanjing Lake.

quantitative analysis, we further validated AVPTW with three natural samples from a contaminated river, Nanfei River. The videos (Supporting Movies 3−5) presented a tendency that species abundances of sites downstream of the outlet (Sites 2 and 3) were substantially richer than those upstream of the wastewater outlet (Site 1). For example, algae were found at Site 3, while Crustacea was found at Site 2 (Figures S14 and S15). The counting results confirm the differences in zooplankton abundance across all sites (Figure 5a−c). The maximum number and frequency of rotifers at Sites 2 and 3 were higher than those at Site 1. This result implies that zooplankton upstream of the outlet were not as abundant as those downstream of the outlet. A possible explanation was that wastewater discharge brought about excess inputs of nutrients[35,36] and thus affected the microbial diversity and motility.

Surprisingly, no substantial difference in fluorescence EEMs at different sites was found (Figure 5d−f). Also, the COD values of the water at the three sites was 92, 110, and 202 mg/L, and the difference might be related to organic pollution. A comparison indicates that AVPTW, via tracking and counting indicators (i.e., zooplankton and phytoplankton), was able to reveal the hidden information about water quality and ecological state of aquatic environments, which could be reflected by neither COD nor fluorescence EEMs. Tracking and counting zooplankton and phytoplankton may play a great role in water quality evaluation.

Monitoring the Variation of Multiple Classes of Plankton with Simulated Wastewater Discharge. In conventional environmental monitoring, it is difficult to detect sudden pollution, especially via manually counting plankton with microscopy. Two natural samples were used to imitate sudden pollution and examine the performance of AVPTW.

https://doi.org/10.1021/acs.est.3c00253
Environ. Sci. Technol. XXXX, XXX, XXX−XXX

The samples from Nanfei River contained more zooplankton, allowing the workflow to detect a higher quantity of rotifers before dosing industrial wastewater. Before and after dosing industrial wastewater, the statistical results of rotifer densities for each injection were compared. Rotifers were found in over 90% of tests before dosing wastewater, while rotifers did not appear in 77.1% of injections after dosing wastewater (Figure 6a,b). Both the quantity and frequency of rotifers deceased after dosing wastewater, preliminarily suggesting the toxic effects of wastewater on rotifers. To give a realistic picture of environmental changes, plankton identification should not be limited to only one or two species of plankton. Multiple phytoplankton and zooplankton could complement each other; thus, monitoring the population response of multiple plankton species could facilitate the unraveling of complex environmental stressors.

We directly tested the water samples from Yanjing Lake at our campus using AVPTW. Multiple classes of zooplankton and phytoplankton were tracked (Figure S16). Decreases in quantity and frequency were observed for the majority of classes after dosing wastewater. For Euglenidae, Trachelophyllidae, Rotifer, and Haematococcus, lower densities occurred more frequently than those in the uncontaminated water samples. Statistical results also confirm that the mean abundance before dosing was larger than that after dosing for most classes, especially for Euglenidae and Rotifer (Figure 6c−h). The initial average abundance of Euglenidae was 7352.76 ind/L higher than the subsequent average abundance. For Rotifer, it was 1450.58 ind/L. However, Parameciidae and Litonotidae showed exceptions: no significant reduction in abundance was found compared with the other classes (Figure 6c,f). Compared with the expectations, Parameciidae and Litonotidae appeared to be unaffected by contamination. These findings could be attributed to the difference in their sensitivity to pollution, indicating that each class of zooplankton and phytoplankton diversely responded to sudden contamination.

Notably, tests within high temporal density could not only guarantee the reliability of counting results but also monitor changes in the abundance of diverse microfauna and phytoplankton at a time scale. Overall, AVPTW is applicable for both single and multiclass with low abundance. Thus, AVPTW is a robust approach to reflect changes in water quality.

Environmental Implications. Plankton are widely distributed in aquatic environments, especially in rivers, oceans, and wastewater treatment plants. Plankton not only play an important role in the ecosystem but also serve as a sensitive biological indicator for water quality. Although deep learning has been demonstrated for planktonic identification with images, image-based plankton detection is still challenging for statistics and online monitoring in natural samples because of the limited image quantity, the small-bodied appearance, and the swimming nature of plankton.

Our work provides a video-oriented automated reproducible workflow, AVPTW, to solve these problems. By calibrating and analyzing the accurate trajectory of moving plankton in videos, living plankton can be well counted in different types of water bodies. Profoundly, AVPTW can monitor the abundance of living plankton at temporal and spatial scales and acutely capture abundance changes in the aquatic environment. Thus, AVPTW can provide long-term continuous monitoring for the actual water body *in situ*. Additionally, the reliability and accuracy of AVPTW make it well-suited for use in various environments and conditions, further expanding its potential applications. Our results also suggest that data augmentation contributes to the amplification of available images and labels, while a large input network image size can provide a significant improvement in the identification of small plankton. Although plankton are widely considered a sensitive indicator of environmental change and contamination,[37,38] a further understanding of the variations in some plankton species remains challenging.[39] This could be achieved by long-term continuous monitoring and correlation analysis based on machine learning. This work also suggested that data science for environmental monitoring should focus not only on developing novel deep-learning frameworks but also on acquiring a large amount of data from the real world. Cost-effectiveness (less than 60 $) makes AVPTW suitable for environmental monitoring tasks that require the collection of a large amount of data points. By allowing researchers to gather more extensive and detailed data sets, it can aid in identifying patterns and trends that would otherwise be challenging to detect. This, in turn, can support better decision-making and policy development. By leveraging cost-effective and mobile data acquisition hardware, "big data" analysis can handily acquire sufficient data support, so that deep learning can be widely applied for environmental monitoring.

■ ASSOCIATED CONTENT

Supporting Information

The Supporting Information is available free of charge at https://pubs.acs.org/doi/10.1021/acs.est.3c00253.

Schematic of the homemade continuous injection device, confusion matrix of models trained by different methods, val batch 0, batch 1, and batch 2, of different methods, train batch 0 before and after data augmentation, train batch 1 before and after data augmentation, train batch 2 before and after data augmentation, information about labels in the training set before and after data augmentation, species found at site 2 and site 3 of Nanfei River by AVPTW, and plankton density of water samples from Yanjing Lake before and after adding industrial wastewater (PDF)

Misidentification of rotifer as paramecium (MP4)

Misidentification of paramecium as rotifer (MP4)

Video of natural water samples from Nanfei River at site 1 by AVPTW (MP4)

Video of natural water samples from Nanfei River at site 2 by AVPTW (MP4)

Video of natural water samples from Nanfei River at site 3 by AVPTW (MP4)

■ AUTHOR INFORMATION

Corresponding Authors

Chen Qian − *CAS Key Laboratory of Urban Pollutant Conversion, Department of Environmental Science and Engineering, University of Science and Technology of China, Hefei 230026, People's Republic of China;* orcid.org/0000-0002-5444-9968; Email: qianc@ustc.edu.cn

Han-Qing Yu − *CAS Key Laboratory of Urban Pollutant Conversion, Department of Environmental Science and Engineering, University of Science and Technology of China, Hefei 230026, People's Republic of China;* orcid.org/0000-0001-5247-6244; Email: hqyu@ustc.edu.cn

Authors

Zhuo Chen − *CAS Key Laboratory of Urban Pollutant Conversion, Department of Environmental Science and Engineering, University of Science and Technology of China, Hefei 230026, People's Republic of China*

Meng Du − *CAS Key Laboratory of Urban Pollutant Conversion, Department of Environmental Science and Engineering, University of Science and Technology of China, Hefei 230026, People's Republic of China*

Xu-Dan Yang − *CAS Key Laboratory of Urban Pollutant Conversion, Department of Environmental Science and Engineering, University of Science and Technology of China, Hefei 230026, People's Republic of China*

Wei Chen − *School of Metallurgy and Environment, Central South University, Changsha 410083, People's Republic of China;* orcid.org/0000-0002-1812-8112

Yu-Sheng Li − *CAS Key Laboratory of Urban Pollutant Conversion, Department of Environmental Science and Engineering, University of Science and Technology of China, Hefei 230026, People's Republic of China; Institute of Advanced Technology, University of Science and Technology of China, Hefei 230031, People's Republic of China*

Complete contact information is available at: https://pubs.acs.org/10.1021/acs.est.3c00253

Notes

The authors declare no competing financial interest.

■ ACKNOWLEDGMENTS

We thank the National Natural Science Foundation of China (52170056, 51821006, 52192684, and 52170057), the Program for Changjiang Scholars and Innovative Research Team at the University of the Ministry of Education of China, and the Fundamental Research Funds for the Central Universities for supporting this work.

■ REFERENCES

(1) Furnas, M.; Mitchell, A.; Skuza, M.; Brodie, J. In the other 90%: phytoplankton responses to enhanced nutrient availability in the Great Barrier Reef Lagoon. *Mar. Pollut. Bull.* **2005**, *51*, 253−265.

(2) Falkowski, P. Ocean Science: The power of plankton. *Nature.* **2012**, *483*, S17−S20.

(3) Zhang, T.; Ma, H.; Hong, Z. C.; Fu, G. Q.; Zheng, Y.; Li, Z.; Cui, F. Y. Photo-reactivity and photo-transformation of algal dissolved organic matter unraveled by optical spectroscopy and high-resolution mass spectrometry analysis. *Environ. Sci. Technol.* **2022**, *56*, 13439−13448.

(4) Barsanti, L.; Birindelli, L.; Gualtieri, P. Water monitoring by means of digital microscopy identification and classification of microalgae. *Environ. Sci-Proc. Imp.* **2021**, *23*, 1443−1457.

(5) Cole, M.; Lindeque, P.; Fileman, E.; Halsband, C.; Goodhead, R.; Moger, J.; Galloway, T. S. Microplastic Ingestion by Zooplankton. *Environ. Sci. Technol.* **2013**, *47*, 6646−6655.

(6) Botterell, Z. L. R.; Beaumont, N.; Cole, M.; Hopkins, F. E.; Steinke, M.; Thompson, R. C.; Lindeque, P. K. Bioavailability of Microplastics to Marine Zooplankton: Effect of Shape and Infochemicals. *Environ. Sci. Technol.* **2020**, *54*, 12024−12033.

(7) Caumette, G.; Koch, I.; Estrada, E.; Reimer, K. J. Arsenic speciation in plankton organisms from contaminated lakes: Transformations at the base of the freshwater food chain. *Environ. Sci. Technol.* **2011**, *45*, 9917−9923.

(8) Boyer, J. N.; Kelble, C. R.; Ortner, P. B.; Rudnick, D. T. Phytoplankton bloom status: Chlorophyll a biomass as an indicator of water quality condition in the southern estuaries of Florida, USA. *Ecol. Indic.* **2009**, *9*, S56−S67.

(9) Shi, K.; Zhang, Y. L.; Zhang, Y. B.; Li, N.; Qin, B. Q.; Zhu, G. W.; Zhou, Y. Q. Phenology of Phytoplankton Blooms in a Trophic Lake Observed from Long-Term MODIS Data. *Environ. Sci. Technol.* **2019**, *53*, 2324−2331.

(10) Bhattacharya, R.; Osburn, C. L. Multivariate analyses of phytoplankton pigment fluorescence from a freshwater river network. *Environ. Sci. Technol.* **2017**, *51*, 6683−6690.

(11) Jha, M. K.; Shekhar, A.; Jenifer, M. A. Assessing groundwater quality for drinking water supply using hybrid fuzzy-GIS-based water quality index. *Water Res.* **2020**, *179*, 115867.

(12) Barcellos, D. D.; de Souza, F. T. Optimization of water quality monitoring programs by data mining. *Water Res.* **2022**, *221*, 118805.

(13) Owen, R. W. Microscale and fine-scale variations of small plankton in coastal and pelagic environments. *J. Mar. Res.* **1989**, *47*, 197−240.

(14) Kyathanahally, S. P.; Hardeman, T.; Merz, E.; Bulas, T.; Reyes, M.; Isles, P.; Pomati, F.; Baity-Jesi, M. Deep learning classification of lake zooplankton. *Front. Microbiol.* **2021**, *12*, 746297.

(15) Chen, W. Y.; Zhao, Y. Y.; You, T. F.; Wang, H. F.; Yang, Y.; Yang, K. Automatic detection of scattered garbage regions using small unmanned aerial vehicle low-altitude remote sensing images for high-altitude natural reserve environmental protection. *Environ. Sci. Technol.* **2021**, *55*, 3604−3611.

(16) Villon, S.; Mouillot, D.; Chaumont, M.; Darling, E. S.; Subsol, G.; Claverie, T.; Villeger, S. A deep learning method for accurate and fast identification of coral reef fishes in underwater images. *Ecol. Inform.* **2018**, *48*, 238−244.

(17) Pedraza, A.; Bueno, G.; Deniz, O.; Ruiz-Santaquiteria, J.; Sanchez, C.; Blanco, S.; Borrego-Ramos, M.; Olenici, A.; Cristobal, G. Lights and pitfalls of convolutional neural networks for diatom identification. *Proceedings of the SPIE Photonics Europe: Optics, Photonics and Digital Technologies for Imaging Applications*; April 22−26, 2018; SPIE: 2018; *10679*.

(18) Lumini, A.; Nanni, L. Deep learning and transfer learning features for plankton classification. *Ecol. Inform.* **2019**, *51*, 33−43.

(19) Krause, L. M. K.; Koc, J.; Rosenhahn, B.; Rosenhahn, A. Fully convolutional neural network for detection and counting of diatoms on coatings after short-term field exposure. *Environ. Sci. Technol.* **2020**, *54*, 10022−10030.

(20) Merz, E.; Kozakiewicz, T.; Reyes, M.; Ebi, C.; Isles, P.; Baity-Jesi, M.; Roberts, P.; Jaffe, J. S.; Dennis, S. R.; Hardeman, T.; Stevens, N.; Lorimer, T.; Pomati, F. Underwater dual-magnification imaging for automated lake plankton monitoring. *Water Res.* **2021**, *203*, 117524.

(21) Kerr, T.; Clark, J. R.; Fileman, E. S.; Widdicombe, C. E.; Pugeault, N. Collaborative deep learning models to handle class imbalance in flowcam plankton imagery. *Ieee Access.* **2020**, *8*, 170013−170032.

(22) Gorsky, G.; Ohman, M. D.; Picheral, M.; Gasparini, S.; Stemmann, L.; Romagnan, J. B.; Cawood, A.; Pesant, S.; Garcia-Comas, C.; Prejger, F. Digital zooplankton image analysis using the ZooScan integrated system. *J. Plankton. Res.* **2010**, *32*, 285−303.

(23) Olson, R. J.; Sosik, H. M. A submersible imaging-in-flow instrument to analyze nano-and microplankton: Imaging FlowCytobot. *Limnol. Oceanogr-Meth.* **2007**, *5*, 195−203.

(24) Redmon, J.; Divvala, S.; Girshick, R.; Farhadi, A. *You only look once: Unified, real-time object detection: Conference on Computer Vision and Pattern Recognition (CVPR)*; IEEE: 2016; pp 779−788.

(25) Ultralytics. YOLOv5. Available online: https://github.com/ultralytics/yolov5 (accessed on 28 September 2022).

(26) Du, Y.; Song, Y.; Yang, B.; Zhao, Y. Strongsort: make deepsort great again. *IEEE Trans. Multimedia* **2023**, 1.

(27) Liu, L.; Ouyang, W. L.; Wang, X. G.; Fieguth, P.; Chen, J.; Liu, X. W.; Pietikainen, M. Deep learning for generic object detection: A survey. *Int. J. Comput. Vision.* **2020**, *128*, 261−318.

(28) Devries, T.; Taylor, G. W. Improved regularization of convolutional neural networks with cutout. *ArXiv.* 2017, *1708.04552*.

(29) Wojke, N.; Bewley, A.; Paulus, D. Simple online and realtime tracking with a deep association metric. *IEEE International Conference*

on Image Processing ICIP:24th IEEE International Conference on Image Processing (ICIP); IEEE: 2017; pp 3645−3649.
(30) Girshick, R. Fast R-CNN. *IEEE International Conference on Computer Vision: IEEE International Conference on Computer Vision*; IEEE: 2015; pp 1440−1448.
(31) Yu, F. B.; Wei, C. H.; Deng, P.; Peng, T.; Hu, X. G. Deep exploration of random forest model boosts the interpretability of machine learning studies of complicated immune responses and lung burden of nanoparticles. *Science Advances.* **2021**, *7*, No. eabf4130.
(32) Goodwin, M.; Halvorsen, K. T.; Jiao, L.; Knausgard, K. M.; Martin, A. H.; Moyano, M.; Oomen, R. A.; Rasmussen, J. H.; Sordalen, T. K.; Thorbjornsen, S. H. Unlocking the potential of deep learning for marine ecology: overview, applications, and outlook. *Ices J. Mar. Sci.* **2022**, *79*, 319−336.
(33) Wang, G.; Song, M.; Hwang, J.-N. Recent advances in embedding methods for multi-object tracking: a survey. *ArXiv.* 2022; 2205.10766.
(34) Oie, G.; Olsen, Y. Influence of rapid changes in salinity and temperature on the mobility of the rotifer brachionus-plicatilis. *Hydrobiologia.* **1993**, *255*, 81−86.
(35) Weitere, M.; Altenburger, R.; Anlanger, C.; Baborowski, M.; Bärlund, I.; Beckers, L.-M.; Borchardt, D.; Brack, W.; Brase, L.; Busch, W.; Chatzinotas, A.; Deutschmann, B.; Eligehausen, J.; Frank, K.; Graeber, D.; Griebler, C.; Hagemann, J.; Herzsprung, P.; Hollert, H.; Inostroza, P. A.; Jäger, C. G.; Kallies, R.; Kamjunke, N.; Karrasch, B.; Kaschuba, S.; Kaus, A.; Klauer, B.; Knöller, K.; Koschorreck, M.; Krauss, M.; Kunz, J. V.; Kurz, M. J.; Liess, M.; Mages, M.; Müller, C.; Muschket, M.; Musolff, A.; Norf, H.; Pöhlein, F.; Reiber, L.; Risse-Buhl, U.; Schramm, K.-W.; Schmitt-Jansen, M.; Schmitz, M.; Strachauer, U.; von Tümpling, W.; Weber, N.; Wild, R.; Wolf, C.; Brauns, M. Disentangling multiple chemical and non-chemical stressors in a lotic ecosystem using a longitudinal approach. *Sci. Total Environ.* **2021**, *769*, 144324.
(36) Woodward, G.; Gessner, M. O.; Giller, P. S.; Gulis, V.; Hladyz, S.; Lecerf, A.; Malmqvist, B.; McKie, B. G.; Tiegs, S. D.; Cariss, H.; Dobson, M.; Elosegi, A.; Ferreira, V.; Graca, M. A. S.; Fleituch, T.; Lacoursiere, J. O.; Nistorescu, M.; Pozo, J.; Risnoveanu, G.; Schindler, M.; Vadineanu, A.; Vought, L. B. M.; Chauvet, E. Continental-scale effects of nutrient pollution on stream ecosystem functioning. *Science.* **2012**, *336*, 1438−1440.
(37) Komarovsky, B. A cladoceran from the plankton as a possible indicator for the presence of the nile flood off the Israeli coast. *Nature.* **1953**, *171*, 937−937.
(38) Verlecar, X. N.; Desai, S. R.; Sarkar, A.; Dalal, S. G. Biological indicators in relation to coastal pollution along Karnataka coast, India. *Water Res.* **2006**, *40*, 3304−3312.
(39) Bedford, J.; Ostle, C.; Johns, D. G.; Atkinson, A.; Best, M.; Bresnan, E.; Machairopoulou, M.; Graves, C. A.; Devlin, M.; Milligan, A.; Pitois, S.; Mellor, A.; Tett, P.; McQuatters-Gollop, A. Lifeform indicators reveal large-scale shifts in plankton across the North-West European shelf. *Global. Change. Biol.* **2020**, *26*, 3482−3497.

https://doi.org/10.1021/acs.est.3c00253
Environ. Sci. Technol. XXXX, XXX, XXX−XXX